Supporting Information

Developing a sharp cone warhammer-like MIL-88A/Ag/MIL-88B Z-scheme heterojunction by controlled in situ semi-conversion strategy: Adsorption-photodegradation of meloxicam and antibacterial activity

Di Sun[a,c,#], Xinru Lin[c,#], Zonghe Yu[c], Xingbin Li[a], Peng Yan[a,*], Yang Wang[b,*], Yuzhong Gao[a,*]

[a] *Department of Orthopedics, First Affiliated Hospital of Jinzhou Medical University, Jinzhou, PR China*

[b] *Research Center for Biomedical Materials, Shenyang Key Laboratory of Biomedical Polymers, Engineering Research Center of Ministry of Education for Minimally Invasive Gastrointestinal Endoscopic Techniques, Shengjing Hospital of China Medical University, Shenyang, PR China*

[c] *School of Pharmaceutical Science, Liaoning University, Shenyang, PR China*

Corresponding author.

E-mail: yanpengky@126.com (P. Yan), wangyang926@sj-hospital.org (Y. Wang), gaoyz@jzmu.edu.cn (Y. Gao).

1.Materials

Ferric chloride hexahydrate ($FeCl_3·6H_2O$, AR), potassium chloride (KCl, AR), anhydrous calcium chloride ($CaCl_2$, AR) were provided by Sinopharm Chemical Reagent Co., Ltd. Terephthalic acid (BCD, AR) was purchased from Shanghai Macklin Biochemical Co., Ltd. Sodium hydroxide (NaOH, AR) and sodium sulfate (Na_2SO_4, AR) were purchased from Tianjin Best Chemical Co., Ltd. Ethanol (C_2H_5OH, AR) and N, N-dimethylformamide (DMF, AR) were provided by Tianjin Hengxing Chemical reagent manufacturing Co., Ltd. Methanol (CH_3OH, AR) and magnesium chloride hexahydrate ($MgCl_2·6H_2O$, AR) from Tianjin Damao chemical reagent factory. Silver nitrate ($AgNO_3$, AR) comes from Nanjing Chemical Reagent Co., Ltd. Fumaric acid (FA, AR) was purchased from Maya Reagents Ltd. Meloxicam (MLX, AR) from Wuhan Xinweiye Chemical Co., Ltd. Sodium sulfite (Na_2SO_3, AR), sodium chloride (NaCl, AR) and Mannitol (D-man, AR) were purchased from Tianjin Yongda Chemical reagent Co., Ltd. Sodium carbonate (Na_2CO_3, AR) was supplied by Tianjin Bodi Chemical Co., Ltd. LB Broth was provided from Hangzhou Best Biotechnology Co., Ltd. Nutrient Agar from Beijing Aoboxing Biotechnology Co., Ltd. The Escherichia coli (E. coli, ATCC 25922), Staphylococcus aureus (S. aureus, ATCC 6538) and methicillin-resistant Staphylococcus aureus (MRSA, ATCC 43300) were provided by Shanghai Luwei Technology Co., Ltd.

2.Instruments

The elemental composition and surface chemical valence states of catalyst were characterized by X-ray photoelectron spectroscopy (XPS; K-Alpha, USA). The surface area (BET) model of the samples composite materials was studied, and the N_2 gas adsorption desorption isotherms was measured on the Autosorp-MP-iQ-C nitrogen adsorption desorption instrument (USA). The pore volume and size distribution curves of the obtained material were calculated from the desorption branch of the N_2 adsorption desorption isotherm that using the N_2 adsorption desorption isotherm method. The UV visible diffuse reflectance spectra were collected on the UV-2550 UV-Vis spectrophotometer (Japan). Mott Schottky and AC impedance testing were measured on an electrochemical workstation. Photoluminescence (PL) spectra were prepared the F-7000 fluorescence spectrophotometer (Japan). The MLX solution after photodegradation was analyzed a tandem four stage rod time-of-flight liquid chromatography-mass spectrometry (HPLC-MS; Agilent 6530, USA). The phase characterization of the samples were measured on an X-ray powder diffractometer (XRD; D8Advance, Germany) instrument with Cu Kα radiation (λ=0.154 nm), and scanning rate of 10° min^{-1} in the 2θ ranges from 5° to 70°. The material was dispersed in anhydrous ethanol and dripped onto a silicon wafer. After the wafers were allowed to dry naturally, they were glued to the sample stage with conductive adhesive. Subsequently, the samples were subjected to gold spraying and their morphology and microstructure were investigated using a scanning electron microscope (SEM; SU8010, Germany). The

material was dispersed in anhydrous ethanol and dripped onto a copper grid. After the copper mesh was dried, the samples were studied using an ultra-high resolution transmission electron microscope (TEM; JEM2100, Japan).

3. Electrochemical properties

The basic equation for estimating bandgap energy is the Tauc equation:

$$\alpha h\nu^{1/n} = A(h\nu - Eg) \quad (1)$$

where α is the absorption coefficient, h is the Plank's constant, A is a parameter that depends on the transition probability, Eg is the band gap energy.

The flat band potential (E_{fb}) and the semiconductor type of M and MIL-88A were studied by the Mott-Schottky plots. Usually, the E_{fb} of a semiconductor can be calculated by the following equations:

p-type

$$\frac{1}{C^2} = \frac{2}{e\varepsilon\varepsilon_0 N_a}\left(-E + E_{fb} - \frac{K_B T}{e}\right) \quad (2)$$

n-type

$$\frac{1}{C^2} = \frac{2}{e\varepsilon\varepsilon_0 N_d}\left(E - E_{fb} - \frac{K_B T}{e}\right) \quad (3)$$

where e denotes the dielectric constant of the used sample and e_0 is the electric permittivity of the vacuum. N_a, N_d, K_B, T, e, E and C represent acceptor density, donor density, Boltzamann constant, Kelvin temperature, electronic charge, applied potential and space charge capacitance, respectively.

4. Adsorption and photocatalytic performance

Different concentrations of photocatalysts (0.075 g L^{-1}, 0.100 g L^{-1}, 0.125 g L^{-1}, and 0.150 g L^{-1}) were added to 50 mL solution containing MLX (120 mg L^{-1}), then the mixture was stirred in the dark for 30 min. Then, the xenon lamp was stirred and irradiated for 60 min. The concentration of the MLX solution was then analyzed at the absorbance at λ=362 nm (with a UV-2500 spectrophotometer).

The removal efficiency of MLX was calculated by formula:

$$\text{Removal efficiency (\%)} = [(C_0\text{-}C_t)/C_0] \times 100\% \quad (4)$$

Where C_0 and C_t represent the absorbance of MLX at reaction times of 0 and t, respectively.

In order to study the effects of different factors on the degradation of MLX, the experimental conditions were changed as follows: catalyst composite ratio (M, 7AM, MAM-30); MLX concentration (60-160 mg L^{-1}).

Different catalysts (MAM-10, MAM-20, MAM-30, MAM-50 and MAM-70) were added to 0.125g L^{-1} concentration to 50 ml MLX (120 mg L^{-1}). After 30 min of dark adsorption and 60 min of photocatalysis, 2 mL of the solution was filtered and the concentration of MLX was measured by UV spectroscopy. Finally, the removal efficiency of MLX was calculated using formula (4).

In thermodynamics, the experiments are conducted at different temperatures ranging from 293 to 319 K. These studies are mainly aimed at understanding whether the adsorption process is exothermic or endothermic by using enthalpy. Calculations related to enthalpy change (ΔH^o), entropy change (ΔS^o), and Gibb's free energy (ΔG^o)

are also quantified using the standard equations mentioned below. These results can be used to further calculate the spontaneity and feasibility of adsorption, in order to determine the dominant adsorption mechanism in the process of pollutant removal. This will also serve as a verification of the thermodynamic study.

$$\ln\left(\frac{q_e}{C_e}\right) = \frac{\Delta S^o}{R} - \frac{\Delta H^o}{RT} \quad (5)$$

$$\Delta G^o = -RT \cdot \ln\left(\frac{q_e}{C_e}\right) \quad (6)$$

ΔS^o represents the entropy change during the adsorption process (kJ mol^{-1} K^{-1}), ΔH^o is the enthalpy change (kJ mol^{-1}), ΔG^o is the Gibbs free energy (kJ mol^{-1}), R is denoted as the universal gas constant (J mol^{-1} K^{-1}), and T is the temperature (K).

The Langmuir-Hinshelwood (L-H) kinetic model, the formula is as follows:

$$-\ln (C_t/C_0) = k_{app}t \quad (7)$$

where C_0 and C_t are contaminant concentrations at reaction times of 0 and t, respectively. kapp represents the observed pseudo-first-order constant rate constant.

5. Antibacterial performance

Analysis of Biofilm Disruption and Bacterial Capture by Materials Biofilm Disruption. First, prepare suspensions of E. coli, S. aureus and MRSA with an optical density (OD) of 0.1 was seeded at the bottom of 24-well plates and cultured for 24 h to facilitate biofilm formation. Next, various groups of nanofibers were placed on top of the established biofilm and subjected to light treatment. After 24 hours of treatment, the biofilm was stained with crystal violet, and the absorbance (OD value) was quantified after the dye was dissolved in ethanol.

Intracellular Protein Leakage Measurement. Normal saline and MAM-30 were taken, and each 990 μL was placed in a 5 mL centrifuge tube, and irradiated with ultraviolet light for 30 min. Then 10 μL bacterial suspension (10^6 CFU mL^{-1}) was added, and illuminated with a xenon lamp or placed in darkness for 60 min. The bacteria were centrifuged, and the supernatants were gathered on a 96-well plate. BCA reagent (Beyotime, P0012S) was added to the mixture, which was then incubated in the dark for 30 min. OD of each well was measured at 562 nm using a microplate reader.

Measurement of intracellular nucleic acid leakage. After the same treatment is completed, the bacteria are centrifuged, the supernatant is collected, and then the absorbance is measured at λ=260 nm using the UV-2500 spectrophotometer.

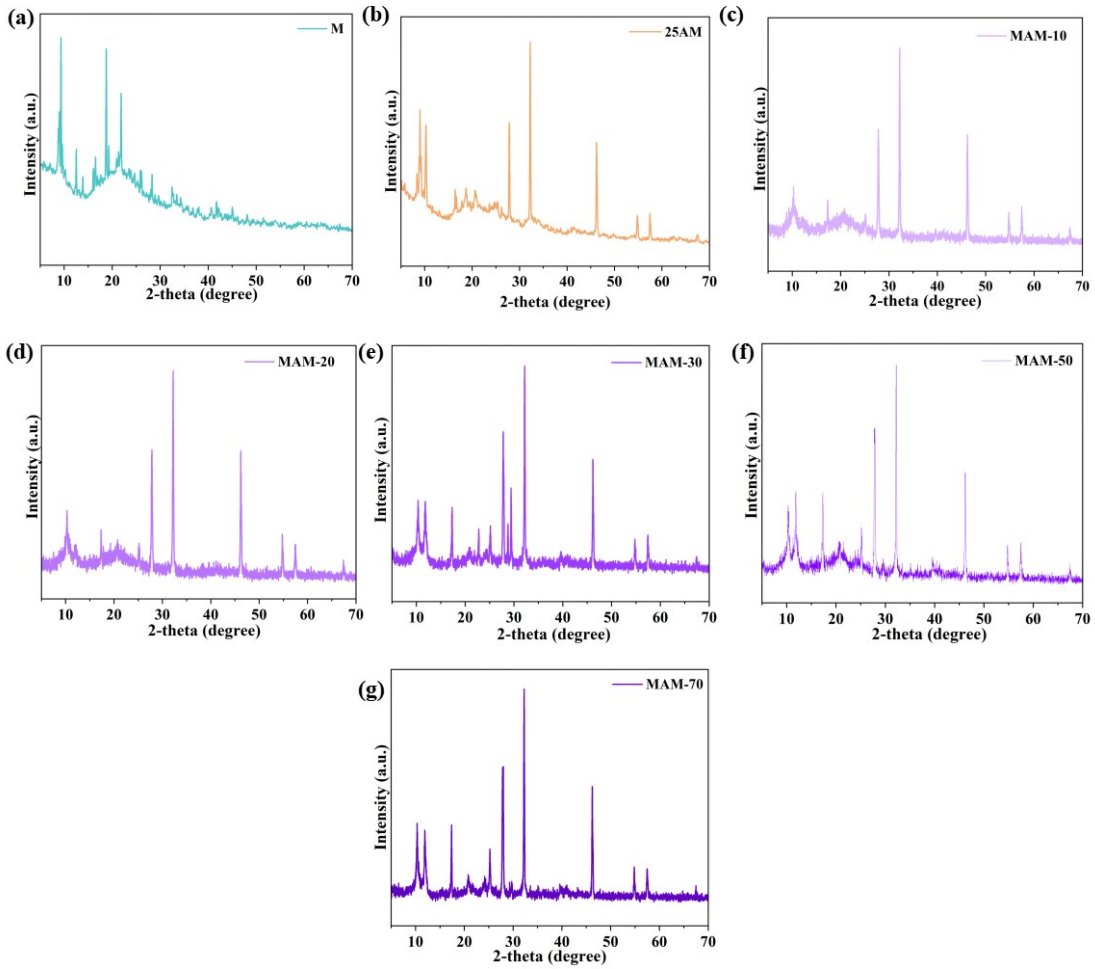

Figure S1. XRD spectrum of M, 7AM, and different reaction times of MAM.

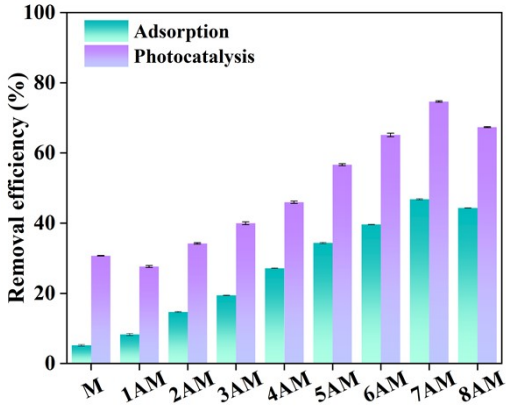

Figure S2. Effect of different composite ratio on MLX removal efficiency.

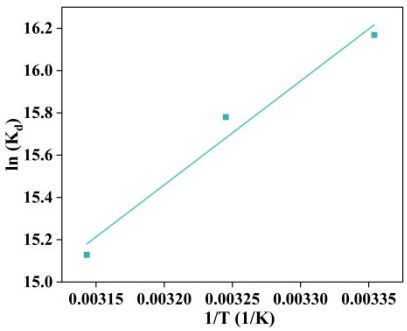

Figure S3. The van't Hoff plot for MLX by MAM-30.

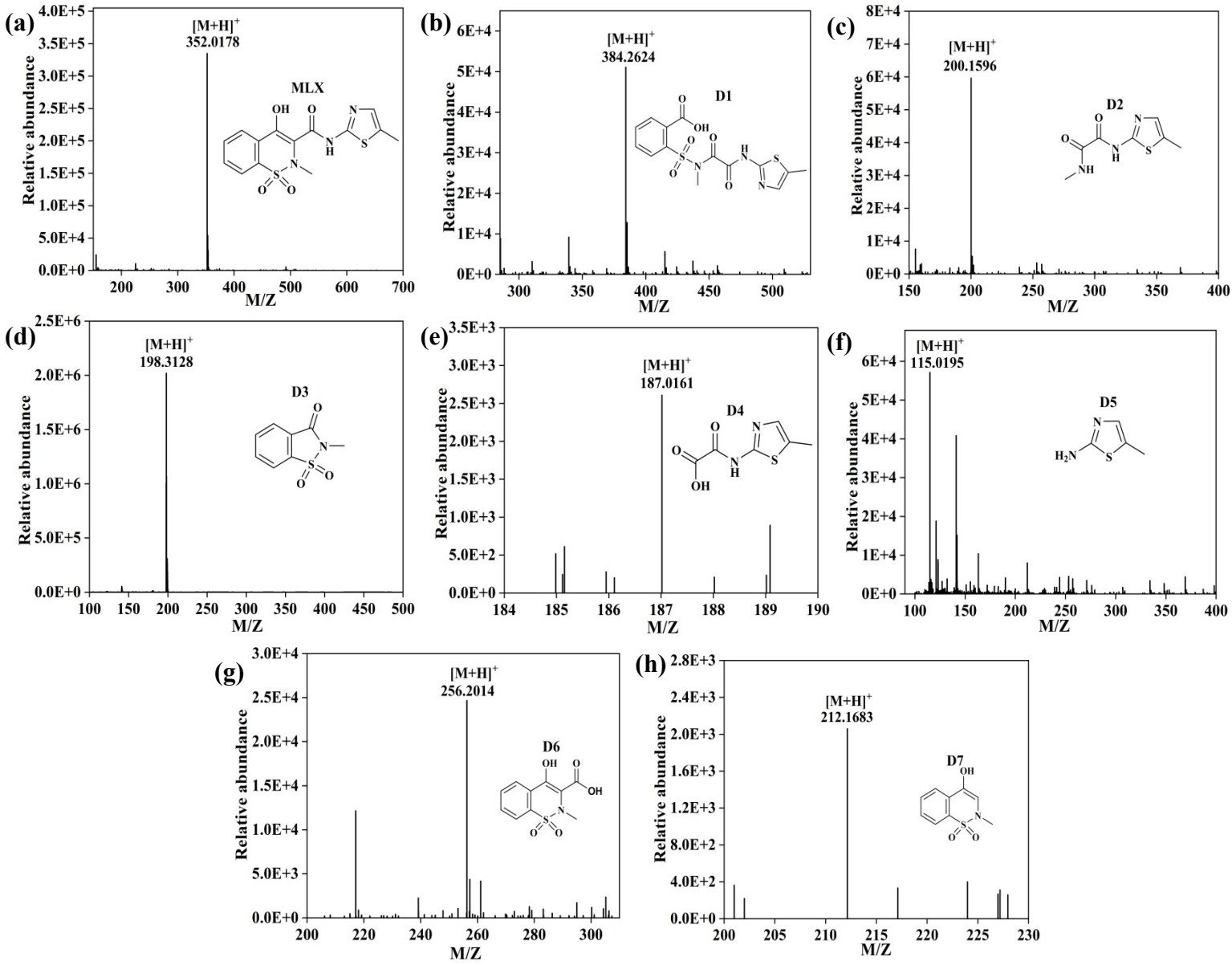

Figure S4. Mass spectra and quasi-molecular ion peaks corresponding to MLX and degradation intermediates.

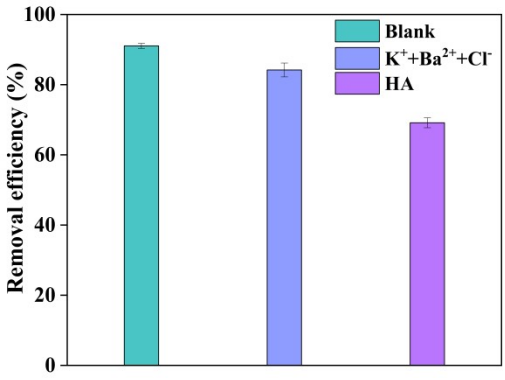

Figure S5. The removal efficiency of MLX by MAM-30 in the presence of mixed ions (K^++Ba^{2+}+Cl^-) and humic acid (HA).

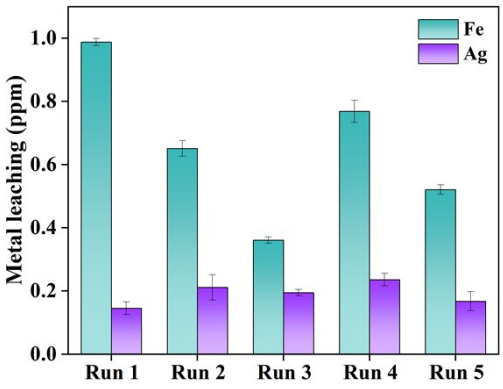

Figure S6. The concentration of dissolved metals after 60 min of photocatalysis in the cyclic experiment.

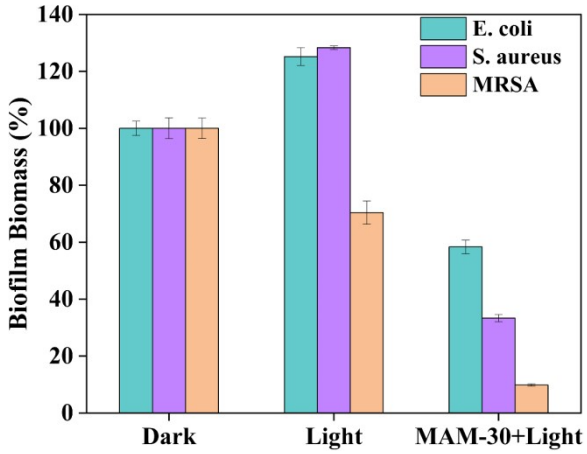

Figure S7. Quantitative measurement of the bacterial biofilm disruption rate.

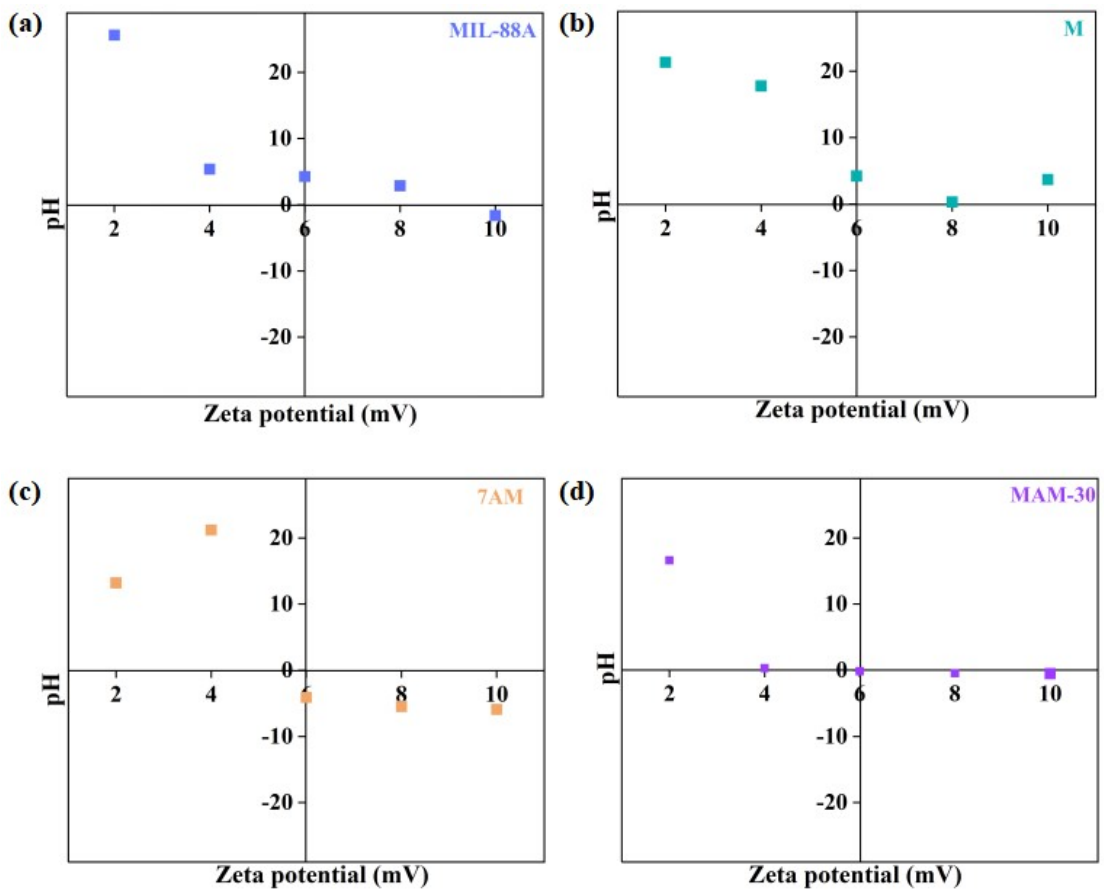

Figure S8. Zeta potential distribution as a function of pH solution of (a) MIL-88A, (b) M, (c) 7AM and (d) MAM-30.

Table S1. The characteristic peaks of MAM-30 in the XRD spectrum correspond to the crystal planes and the material composition.

Samples	2θ (°)	lattice planes	Material composition
MAM-30	9.3	(101)	MIL-88B
	12.5	(102)	
	18.7	(202)	
	21.8	(211)	
	38.1	(111)	Ag
	44.4	(200)	
	8.1	(010)	MIL-88A
	10.4	(100)	
	12.3	(101)	
	15.4	(002)	
	17.4	(012)	

Table S2. Fitting parameters of the Fe 2p and Ag 3d XPS spectrum of MAM-30.

Name		Peak BE	Height CSP	Height Ratio	Area CPS.eV	Area Ratio	FWHM eV	Atomic %
Fe^{2+}	$2p_{3/2}$	711.84	7037.36	1.00	22009.56	2.20	2.00	14.56
	$2p_{1/2}$	724.70	3307.66	0.47	16902.80	1.71	2.00	14.88
Fe^{3+}	$2p_{3/2}$	714.97	3077.25	0.44	17144.34	1.72	1.71	17.44
	$2p_{1/2}$	727.77	1443.56	0.21	7336.33	0.74	2.00	9.70
Ag^0	$3d_{3/2}$	367.5	4420.80	1.00	6124.72	0.32	1.21	47.46
	$3d_{5/2}$	373.4	3159.85	0.71	4138.79	0.22	1.18	31.77
Ag^+	$3d_{3/2}$	368.5	1183.35	0.27	2017.91	0.11	1.19	15.65
	$3d_{5/2}$	374.7	556.24	0.13	861.68	0.05	1.05	5.12

Table S3. Kinetic constants of MLX degradation by MAM-30**.**

Samples	Pseudo-first-order mode $lg(q_e - q_t) = lgq_e - k_1 t$			Pseudo-second-order model $t/q_t = 1/k_2 q_e^2 + t/q_e$		
	k_1 (min^{-1})	q_{e1} (mg g^{-1})	R^2	k_2 (g mg min^{-1})	q_{e2} (mg g^{-1})	R^2
MAM-30	0.0369	1.0065	0.8753	0.2595	0.9555	0.9933

Table S4. Thermodynamic data for the adsorption of MLX on MAM-30.

Pollutant	ΔG^o (kJ mol^{-1})			ΔH^o (kJ mol^{-1})	ΔS^o (kJ mol^{-1} K^{-1})
	298.15K	308.15K	318.15K		
MLX	-40.08	-40.43	-40.02	-40.87	-0.0023

Table S5. The obtained isotherm constants of the MLX removal by MAM-30.

Samples	Langmuir $C_e/Q_e = 1/k_L\ Q_m + C_e/Q_m$			Freundlich $\ln Q_e = \ln k_F + (1/n) \ln C_e$		
	k_L (L mg^{-1})	Q_m (mg g^{-1})	R^2	K_f (mg g^{-1})	n	R^2
MAM-30	0.0012	97.66	0.1710	0.1562	1.0961	0.9544

Table S6. Comparison of the catalytic activities of several published catalysts in MLX degradation.

	Concentration (mg L^{-1})	**Catalyst Dosage (g L^{-1})**	**Time (min)**	**Efficiency (%)**	**Ref.**
$ZnWO_4$	10	1.0	120	75.7	(Xu et al., 2019)
Zeolite/ZnO	100	1	90	75.8	(Sarabyar et al., 2025)
CNS/CQDs	10	0.4	60	96.7	(Wang et al., 2022)
g-C_3N_4/$CaTiO_3$/ CQDs	10	0.4	120	98	(Zhao et al., 2024)
GA-MNP	0.25	12	240	25	(Nadim et al., 2015)
MAM-30	120	0.125	60	96.1	**This work**

Table S7. QSAR prediction the toxicity of MLX and its degradation intermediates for Bioconcentration factor, Developmental toxicity and Mutagenicity toxicity in the process of MLX photodegradation.

By-products	Bioconcentration factor	Developmental toxicity	Mutagenicity
MLX	1.35	0.64	0.1
D1	0.24	0.62	-0.14
D2	0.11	0.65	0.47
D3	2.56	0.78	0.15
D4	0.14	0.62	0.9
D5	2.2	0.63	0.44
D6	0.41	0.99	-0.02
D7	3.37	0.85	0.16

Table S8. Comparison with other similar catalysts for antibacterial activity.

Natural water	**Turbidity (NTU)**	**pH**	**Dissolved oxygen (mg L^{-1})**	**Total Phosphorus (mg L^{-1})**	**Total nitrogen (mg L^{-1})**	**Ammonia nitrogen (mg L^{-1})**	**Manganese Permanganate Index (mg L^{-1})**
Tap water	1.3	8	10.5	0.050	4.92	0.18	2.4
Pu river	6.6	7	13.8	0.015	3.18	0.02	2.3
Hun river	5.1	8	11.2	0.057	5.74	0.69	2.4
Lilac lake	2.0	7	11.5	0.070	10.95	0.16	2.8

Table S9. Comparison with other similar catalysts for antibacterial activity.

Photocatalyst	**Amount (mg mL^{-1})**	**Bacteria suspension concentration (CFU mL^{-1})**	**Time (min)**	**Antibacterial Efficiency (%)**	**Ref.**
2 % F-HKUST-1/PG	0.02	2×10^5	360	58% (*S. aureus*)	(El-Refaie et al., 2024)
Zn-MOF	0.19	10^5	30	90% (*S. aureus*)	(Qing et al., 2024)
9 wt% SA/Co-MOF	50	10^5	120	96.9% (*E. coli*) 99.9% (S. aureus)	(Shao et al., 2023)
PCN-224(Zr/Ti)	0.10	5×10^5	30	96.4% (*E. coli*)	(Chen et al., 2020)
MIL-101(Fe)@Ag	0.1	10^6	120	82% (*E. coli*) 98% (*S. aureus*)	(Xi et al., 2022)
MAM-30	0.02 0.04 0.12	2.5×10^4	60	99.2% (*E. coli*) 98.3% (*S. aureus*) 97.3% *(MRSA)*	**This work**